Fully-CMOS analog and digital SiPMs

Yu Zou[a], Federica Villa[a], Danilo Bronzi[a], Simone Tisa[b], Alberto Tosi[a], Franco Zappa[a,b]
[a]Dip. Elettronica, Informazione e Bioingegneria, Politecnico di Milano, P. Leonardo Da Vinci 32, 20133 Milano, Italy; [b] Micro Photon Device S.r.l., Via Stradivari 4, I-39100, Bolzano, Italy

ABSTRACT

Silicon Photomultipliers (SiPMs) are emerging single photon detectors used in many applications requiring large active area, photon-number resolving capability and immunity to magnetic fields. We present three families of analog SiPM fabricated in a reliable and cost-effective fully standard planar CMOS technology with a total photosensitive area of 1x1 mm^2. These three families have different active areas with fill-factors (21%, 58.3%, 73.7%) comparable to those of commercial SiPM, which are developed in vertical (current flow) custom technologies. The peak photon detection efficiency in the near-UV tops at 38% (fill-factor included) comparable to commercial custom-process ones and dark count rate density is just a little higher than the best-in-class commercial analog SiPMs. Thanks to the CMOS processing, these new SiPMs can be integrated together with active components and electronics both within the microcell and on-chip, in order to act at the microcell level or to perform global pre-processing. We also report CMOS digital SiPMs in the same standard CMOS technology, based on microcells with digitalized processing, all integrated on-chip. This CMOS digital SiPMs has four 32x1 cells (128 microcells), each consisting of SPAD, active quenching circuit with adjustable dead time, digital control (to switch off noisy SPADs and readout position of detected photons), and fast trigger output signal. The achieved 20% fill-factor is still very good.

Keywords: CMOS analog SiPMs, Single photon avalanche diode (SPAD), digital SiPMs, single photon counting, photon number resolved, photon position resolved.

1. INTRODUCTION

In order to detect extremely faint signals, some single-photon detectors have been developed: Photomultiplier Tube (PMT), Microchannel Plate (MCP), Hybrid Photo-Detector (HPD), Superconducting Single-Photon Detector (SSPD), Quantum Dots Single Photon Detector (QDFET), Single-Photon Avalanche Diode (SPAD) and Silicon Photomultiplier (SiPM). Among these, semiconductor devices are strongly preferred for their relatively low bias voltage, insensitive to external magnetic fields, miniature size, rugged, reliable and easy-to-use. SPAD detectors are reverse-biased p-n junction, designed to work above its breakdown voltage in order to exploit the fast and intense avalanche build-up triggered by the absorption of a single optical photon. For single photon detection applications, large area of SPADs have been developed [1], but due to their relatively high Dark Count Rate (DCR) the device is easily saturated by noise. Arrays of SPADs are developed also to provided timing information [2] or for acquisition of very fast 2D imaging with faint signal [3], however, they could not provide the number of simultaneously arriving photons.

SiPMs are large area photodetectors consisting of an array of Single-Photon Avalanche Diodes (SPADs) with passive quenching resistors (analog SiPMs) or active quenching circuits (digital SiPMs), different from SPADs, they provide an analog output which is proportional to firing cells, allowing to discriminate the number of simultaneously arriving photons. High Photon Detection Efficiency (PDE), combined with large collection area, low DCR, SiPMs become extremely useful detectors for many applications, in particular for single photon counting [4][5] and in photon-number resolved [6][7] and multi-photons applications [8]-[10].

The analog SiPMs, each SPAD is connected in series with a quenching resistor that can quench the avalanche by limiting the diode current to a sufficiently low level. All microcells (SPAD and quenching resistor) are connected in parallel, providing an analog output signal by summing the individual currents of all microcells [11]. Instead in digital SiPM SPADs are integrated with conventional CMOS circuits on the same substrate. Each SPAD has its own readout circuit, active quenching and recharging of the SPAD. A one-bit memory cell integrated next to the SPAD can be used to selectively enable or disable the corresponding diode in order to switch off 'hot' (high DCR) SPADs. Each cell is composed by the SPAD itself and by the corresponding electronics blocks [12].

Optical Components and Materials XII, edited by Shibin Jiang, Michel J. F. Digonnet, Proc. of SPIE Vol. 9359, 93591B · © 2015 SPIE · CCC code: 0277-786X/15/$18 · doi: 10.1117/12.2077473

With only passive quenching elements inside each microcell, analog SiPMs provide higher fill-factor with respect to digital SiPMs and special integrated quenching resistors in custom technologies have been designed to further improve fill-factor [13][14]. The exploitation of custom technologies allows optimization the performance of SiPMs, in terms of DCR and PDE; however, it does not allow the integration of complex electronics. To this aim, we designed and fabricated CMOS analog SiPMs based on a standard 0.35 µm technology.

However, analog SiPMs do not fully exploit the excellent intrinsic performance of SPAD. The parasitic capacitances of the on chip interconnect, the bond wires and the external load, degrade the performance of analog SiPMs. A dedicated readout circuit is needed. Furthermore, we need to digitize the analog SiPM signals, as the single photon response is still in the mV range, the signals can be easily affected by electronic noise or unstable baseline due to high DC levels, thus making single photon detection difficult. For these reasons, we designed also an array of digital SiPMs. In digital SiPMs, photons are detected directly by sensing the voltage at the SPAD anode using active quenching circuits. The photons are detected and counts as digital signals, making the sensor less susceptible to noises. In the our designed digital SiPMs, we could selectively enable and disable each microcell and at the end of acquisition, we could also readout the states of each SPAD, thus providing the 2D position information of photons.

This paper is organized as follows: Section 2, we will describe the design of three families of analog SiPMs with different sizes and shapes of SPADs, the characterization of our CMOS analog SiPMs and the comparison with the commercial SiPMs; Section 3, we will present the design of our digital SiPMs; finally, in Section 4, we will make the conclusion of the work.

2. ANALOG SIPMS

2.1 Structure of analog SiPMs

We developed three families of analog SiPMs with different sizes of SPADs in standard 0.35 µm CMOS technology. Each SiPM consists of four macro-pixels with 8x8 microcells each. Inside each macro-pixel, the SPADs' cathodes of each microcells are connected together while the anode of each SPAD is connected to its individual integrated polysilicon quenching resistor, shown in Figure1. The polysilicon quenching resistors (260 kΩ) have been integrated along the four sides of the array, in order to achieve higher FF, with the drawback of limiting the scalability of the device. A unique n-well forms the common cathode for all microcells, as shown in the cross-section of Figure 2.

The three SiPM families have the same structure, the same pitch (58 µm) between adjacent microcells and the same total active area of 928 x 928 μm^2. Three different sizes and shapes of SPADs are designed for each SiPM family: S30 (30 µm round SPADs, FF = 21.0%), S50 (50 µm round SPADs, FF = 58.3%) and S50q (50 µm square SPADs with rounded corners of 5 µm radius, FF = 73.7%). These values of fill-factor are comparable to those of commercial SiPM, which range from 30% (Hamamatsu S12571-010) to 70% (Ketek Standard Technology).

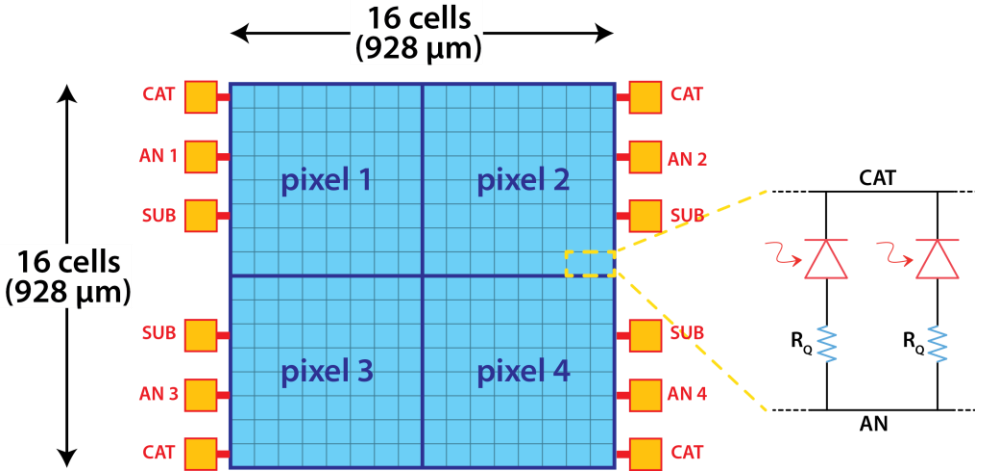

Figure 1. Left: Structure of the SiPM with 16x16 microcells divided into 4 macro-pixels. Right: example of two microcells.

2.2 Characterization of analog SiPMs

We used a transimpedance amplifier connected to the SiPM cathode terminal (Figure 2) to characterize and measure the important SiPM parameters: breakdown voltage, gain, PDE, DCR and crosstalk probability [15]. During the measurements, the four macro-pixels are connected in parallel forming an equivalent 16x16 microcell SiPM. The feedback resistance (R_f=2.2 kΩ) and the feedback capacitance (C_f=2.5 pF) are chosen to obtain proper gain and compensate the stage. The bandwidth of the detector is limited by the stray capacitance of the p-n junction instead of the readout circuit. The total capacitance at the SiPM cathode is tens of pF.

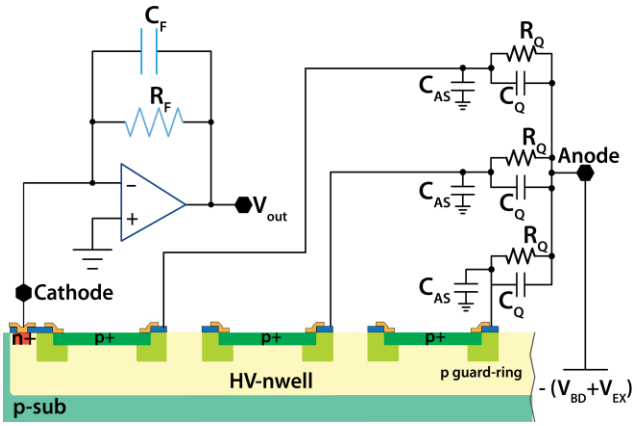

Figure 2. Cross-section of the CMOS SiPM with parasitic capacitances and transimpedance readout circuitry.

The breakdown voltage (V_{BD}) of our SiPMs is about 25 V and we operate the SiPMs at 4V to 6V excess bias voltage (V_{EX}). The gain of SiPM is defined as the intrinsic charge gain of the single microcell and can be computed as:

$$G = \frac{V_{EX} \cdot C_{tot}}{q} = \frac{V_{EX} \cdot (C_{AC} + C_{AS} + C_Q)}{q} \quad (1)$$

where V_{EX} is the excess voltage, C_{AC} is the junction capacitance, C_{AS} is the capacitance between anode and substrate, C_Q is the capacitance in parallel to the quenching resistor and q is the electron charge. All capacitors refer to one single microcell. The gains of three SiPMs families are measured and calculated at 5V excess voltage: $8.8 \cdot 10^6$ (S30), $13.2 \cdot 10^6$ (S50) and $15.0 \cdot 10^6$ (S50q). The higher capacitances value of our SiPMs brings a slightly higher gain with respect to commercial SiPMs ($1 \cdot 10^5$ - $5 \cdot 10^6$). In photon number resolved applications, gain and photoelectron spectrum are key

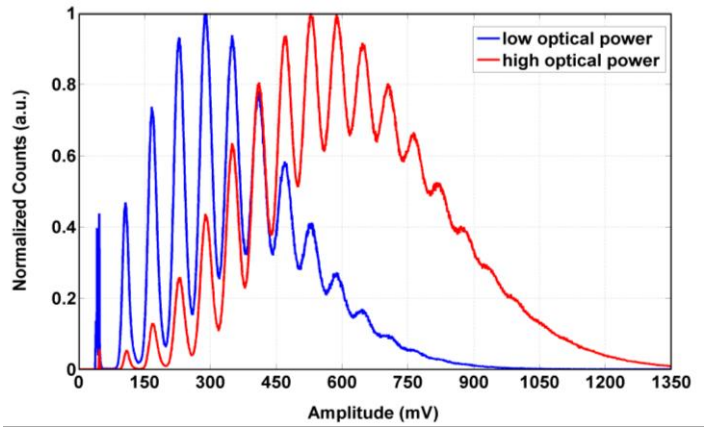

Figure 3. Photoelectron spectrum of a S50q SiPM measured with two different optical power.

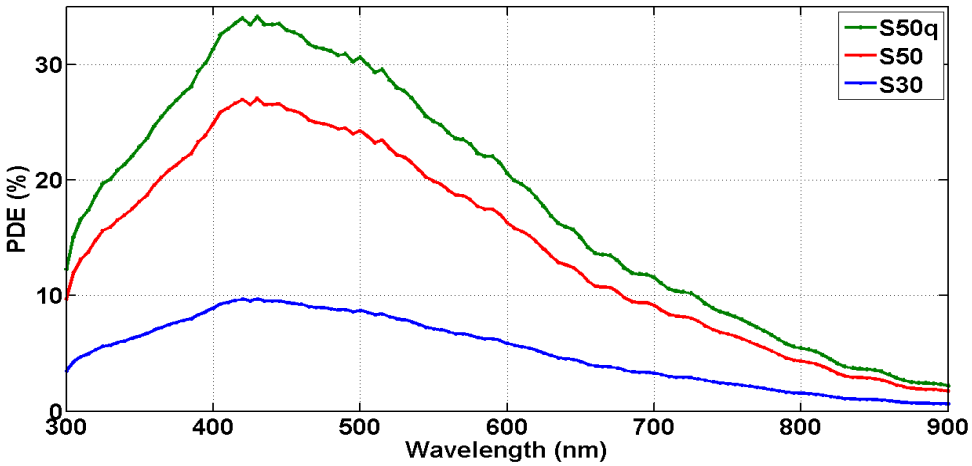

Figure 4. PDE of three developed SiPM with peak values of 10% (S30), 18% (S50) and 38% (S50q).

parameters. Figure 3 shows the photoelectron spectrum of the S50q SiPM measured by multichannel analyzer with two different optical powers and the distinguishable simultaneous photon number is 15. The PDE of our SiPM is calculated by multiplying the measured PDE of single SPAD by the SiPM fill-factor. The SPAD used to measure the PDE has the same size and shape as the SPAD in each microcell, and in fact, these single SPAD and SiPMs are fabricated on the same wafer. The peaks of PDE are located at near UV-region with values of 10%, 18% and 38% shown in Figure 4.

The DCR of SiPMs is the noise contribution of all the microcells and is measured by connecting the output of the transimpedance amplifier to a counter with one-photon level threshold voltage (50 mV) at 5 V of excess voltage. The measured DCR of three SiPMs are 116 kcps (S30), 334 kcps (S50) and 503 kcps (S50q). To compare with commercial SiPMs, the DCR is normalized to the total active area shown in Figure 5. The DCR density of our CMOS SiPM is slightly higher than the best-in-class SiPMs in custom technologies.

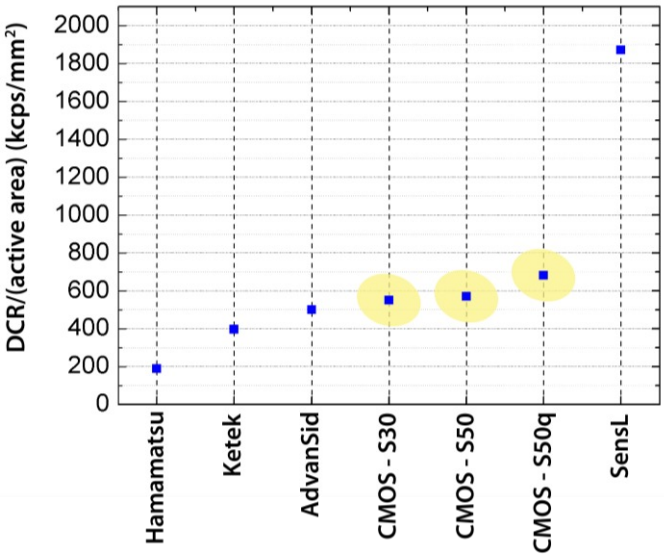

Figure 5. DCR density comparison between commercial custom SiPMs and our CMOS SiPM.

The crosstalk of SiPM is computed as:

$$Xtalk = \frac{DCR_{2p}}{DCR_{1p}} \tag{2}$$

where DCR_{2p} and DCR_{1p} are the DCRs measured with the threshold at two photons and one photon level respectively. The obtained crosstalk probabilities are 18.6% (S30), 23.0% (S50) and 33.5% (S50q), comparable with the no trench isolations custom SiPMs. The crosstalk could be reduced by adding trenches as reported in the literature.

3. DIGITAL SIPMS

We also designed a 32x4 microcells digital SiPMs and these microcells are split into four identical macro-pixels. Figure 6 shows the structure of one macro-pixel and the layout of the whole digital SiPM. Inside each microcell, the anode of SPAD is connected to a variable-load quenching circuit [16] to active quench and recharge the SPAD. Each microcell provides three outputs: one digital voltage output connected in parallel to other microcells, that could go to external TDC [17] for photon arrival time resolving applications or to external counter for photon counting applications; one analog output provides current signal, that gives directly information on simultaneously firing microcells inside each macro-pixel; one digital output to provide the state of one single microcell, which will be registered by a one-bit memory for photon position resolving applications. The one-bit memory is associated to each microcell that could be used to enable and disable the microcell in the configuration phase, and load the state of each microcell at the end of acquisition. The fill-factor of our digital SiPMs is 20% which is still good and by adding the complex electronics elements we could decrease the DCR of the whole SiPMs by switch-off the noisy microcell. At the same time, we exploited the intrinsic properties of SPAD while keep the photon number resolved and photon position resolved capabilities.

4. CONCLUSION

SiPMs are emerging single photon detectors used in many applications requiring large active area and photon number resolving capability. We developed, studied and characterized three families of analog SiPM fabricated in a reliable and cost-effective standard 0.35 µm CMOS technology. These three families have different diameters and shapes of SPAD and with high performance in terms of PDE, DCR and fill-factor comparable to the best commercial analog SiPMs. In order to exploit the intrinsic performance of SPAD, we designed also digital SiPMs with selectable cells, digitalized output, photon number and position resolved capabilities.

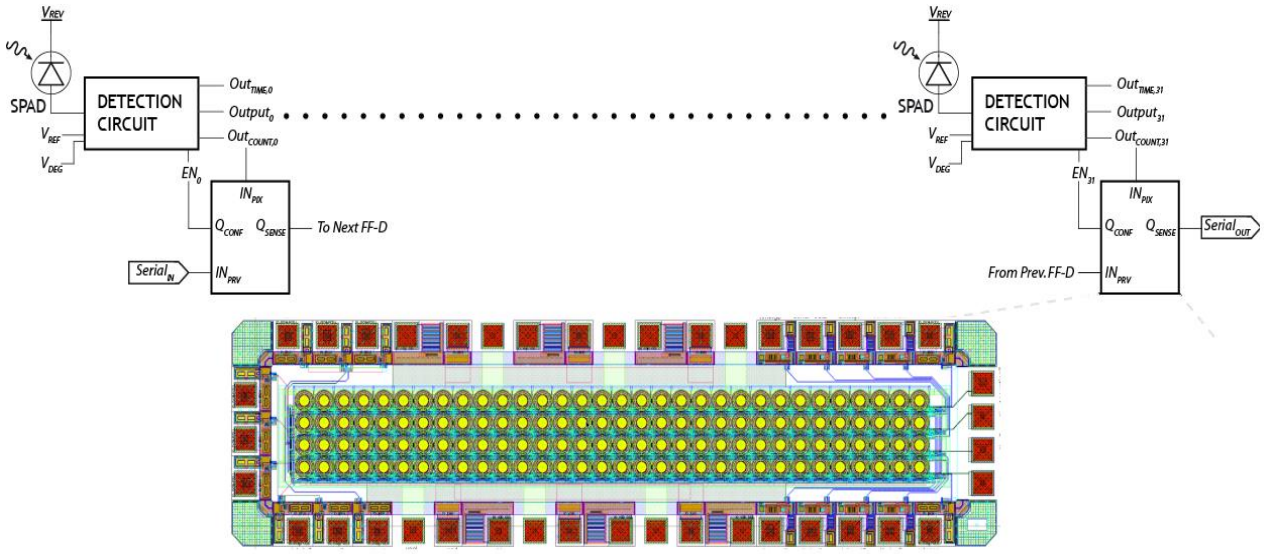

Figure 6. Structure of one macro-pixel (32x1 microcells) of the digital SiPMs and the layout of the SiPM (32x4 microcells).

REFERENCES

[1] Villa, F., Bronzi, D, Zou, Y., Scarcella, C., Boso, G., Tisa, S., Tosi, A., Zappa, F., Durini, D., Weyers, S., Paschen, U. and Brockherde, W., "CMOS SPADs with up to 500 μm diameter and 55% detection efficiency at 420 nm," Journal of Modern Optics 61, pp. 102-115 (2014).

[2] Villa, F., Lussana, R., Bronzi, D.,Tisa, S., Tosi, A., Zappa, F., Dalla Mora, A., Contini, D., Durini, D., Weyers, S. and Brockherde, W., "CMOS Imager With 1024 SPADs and TDCs for Single-Photon Timing and 3-D Time-of-Flight," Selected Topics in Quantum Electronics 20 (6), pp. 364-373 (2014).

[3] Bronzi, D., Villa, F., Tisa, S., Tosi, A., Zappa, F., Durini, D., Weyers, S. and Brockherde, W., "100 000 Frames/s 64 × 32 Single-Photon Detector Array for 2-D Imaging and 3-D Ranging," Selected Topics in Quantum Electronics 20 (6), pp. 354-363 (2014).

[4] Miyamoto, H. and Teshima, H., "SiPM development for the imaging Cherenkov and fluorescence telescopes," Nuclear Instruments and Methods in Physics Research 623 (1), pp. 198-200 (2010).

[5] Zimmermann, R., Braun, F., Achtnich, T., Lambercy, O., Gassert,R. and Wolf, M., "Silicon photomultipliers for improved detection of low light levels in miniature near-infrared spectroscopy instruments," Biomedical Optics Express 4 (5), pp. 659-666 (2013).

[6] Eisaman, M.D., Fan, J., Migdall, A. and Polyakov, S.V., "Single-photon sources and detectors,"Review of Scientific Instruments 82, (2011).

[7] Hadfield, R.H., "Single-photon detectors for optical quantum information applications," Nature Photonics 3 (12), pp. 696-705 (2009).

[8] Beddar, A.S., Mackie, T.R. and Attix, F.H., "Water-equivalent plastic cintillation detectors for High-energy beam dosimetry: I. Physical characteristics and theoretical consideration," Physics in Medicine and Biology 37(10), pp. 1883-1900 (1992).

[9] Herbert, D.J., Moehrs, S., D'Ascenzo, N., Belcari, N., Del Guerra, A., Morsani, F. and Saveliev, V., "The Silicon Photomultiplier for application to high-resolution Positron Emission Tomography," Nuclear Instruments and Methods in Physics Research Section A 573, pp. 84-87 (2007).

[10] Perali, I., Celani, A., Busca, P., Fiorini, C., Marone, A., Basilavecchia, M., Frizzi, T., Roellinghoff, F., Smeets, J., Prieels, D., Stichelbaut, F., Vander Stappen, F., Henrotin, S. and Benilov, A., "Prompt gamma imaging with a slit camera for real-time range control in proton therapy: Experimental validation up to 230 MeV with HICAM and development of a new prototype," IEEE Nuclear Science Symposium Conference Record, pp. 3883-3886 (2012).

[11] Bondarenko, G., Buzhan, P., Dolgoshein, B., Golovin, V., Guschin, E., Ilyin, A., Kaplin, V., Karakash, A., Klanner, R., Pokachalov, V., Popova, E. and Smirnov, K., "Limited Geiger-mode microcell silicon photodiode: new results," Nuclear Instruments and Methods in Physics Research Section A 442, pp.187-192 (2000).

[12] Degenhardt, C., Prescher, G., Frach, T., Thon, A., de Gruyter, R., Schmitz, A. and Ballizany, R., "The digital Silicon Photomultiplier — A novel sensor for the detection of scintillation light," Nuclear Science Symposium Conference Record, pp. 2383-2386 (2009).

[13] Ninković, J., Andriček, L., Liemann, G., Lutz, G., Moser, H.G., Richter, R. and Schopper, F., "SiMPl - an avalanche diode array with bulk integrated quench resistors for single photon-detection," Nuclear Instruments and Methods in Physics Research 617, pp. 407-410 (2010).

[14] Sun, F., Duan, N. and Lo, G.Q., "Novel Silicon Photomultiplier with Vertical Bulk-Si Quenching Resistors," IEEE Electron Device Letters 34, (2013).

[15] Villa, F., Bronzi, D., Vergani, M., Zou, Yu., Ruggeri, A., Zappa, F. and Dalla Mora, A., "Analog SiPM in planar CMOS technology," Solid State Device Research Conference, pp. 294-297 (2014).

[16] Bronzi, D., Tisa, S., Villa, F., Bellisai, S., Tosi, A. and Zappa, F., "Fast Sensing and Quenching of CMOS SPADs for Minimal Afterpulsing Effects," IEEE Photonics Technology Letters 25 (8), pp.776-779 (2013).

[17] Tamborini, D., Portaluppi, D., Villa, F., Tisa, S. and Tosi, A., "Multichannel low power time-to-digital converter card with 21 ps precision and full scale range up to 10 μs," Review of Scientific Instruments 85, 114703 (2014).